II. Rate Studies in Concentrated Solutions

Fixed-bed kinetic studies were made for $Fe^{+++} - H^{+}$ exchange, with perchlorate as the anion, covering concentrations from 0.5 N to 2.0 N in total cation, flow rates of 5 ml./min. sq. cm. to 45 ml./min. sq. cm. bed depth of 25 to 60 cm., and average resin particle diameters of 0.28 and 0.56 mm. The results are correlated on the assumption of internal diffusion as the rate-controlling step and an essentially irreversible equilibrium.

The exchange of ions between the liquid and resin phases in an ion exchange system can be interpreted, and subsequently predicted for design purposes, in terms of well-established mass transfer principles. Thus the three fundamental principles governing cation exchange are conservation of mass, as expressed by a material balance; the law of mass action, represented by the equilibrium relationships between ions in solution and on the resin phase; and the rate of mass transfer between the liquid and resin phases. Although considerable attention has been given in recent years to the elucidation and application of these principles for ion exchange processes, especially from a theoretical viewpoint, large areas exist for which experimental studies are lacking to verify proposed theories and equations or to provide the data needed to use available theory for design of commercial units. One such area is polyvalent—univalent cation exchange at high concentrations. Part I has presented the equilibrium relationships for a system of this type, the $Fe^{+++} - H^{+}$ exchange. The present paper deals with rate studies in fixed beds for this same system, at solution concentrations from 0.5 to 2.0 N in Fe^{+++} content.

PERTINENT THEORY

Fixed beds were employed in the present study both because this experimental method appeared to be best adapted to working with concentrated solutions of the type under study and because the majority of commercial ion exchange operations employ fixed-bed units, or moving-bed units to which fixed-bed theory is applicable (*1*, *9*). In fixed-bed studies the concentrations of the exchanging ions in the effluent from the bed are related to operating variables such as the entering solution composition and concentration, the mass flow rate through the bed, the bed size, and the exchange-material particle size. If possible, the effluent concentration is related to these variables by an equation termed the *breakthrough* equation. Breakthrough equations are obtained by the combination of the proper equations for the fundamental principles governing ion exchange, as listed above, into a partial differential equation defining the ion exchange process in a differential length of the bed. This differential equation is then solved with the boundary conditions conforming to the operating variables of the particular system under consideration. An exact generalized breakthrough equation covering all possible cases of fixed-bed ion exchange is not feasible, partly because of the wide variety of equilibria encountered in ion exchange. Another factor rendering generalization difficult is that the rate of exchange in fixed beds may be controlled by diffusion of any of the exchanging ions through the liquid film surrounding the resin particle, through the solution within the pores of the resin particle (internal diffusion), or by a combination of these two diffusional processes (*3*). An approximate generalized solution, based on various simplifying assumptions, has recently been presented graphically (*5*), but in the present study it was found more convenient to employ breakthrough equations specifically applicable to the system being studied.

As discussed in Part I, the equilibrium for the $Fe^{+++} - H^{+}$ exchange is such that the exchange of iron onto the resin is always highly favored. Previous studies have also indicated that, with the concentrated solutions being employed in the present study, diffusion within the pores of the resin would be the rate-controlling step in the exchange process (*3*). For the similar conditions of irreversible equilibria, internal diffusion rate controlling, Vermeulen (*11*) has shown that at a given instant the exchange of ions in a fixed bed occurs within a fairly small length of the bed. This exchanging zone, once formed, then moves down the bed at a constant rate and with constant thickness. In the exchange zone the surface of the resin particles becomes and remains saturated with the incoming ion as soon as solution containing this ion reaches a particle (material-balance conditions permitting). Thereafter transfer of incoming ions to the particle is limited by the rate at which ions can diffuse within the pores of the particle, a process defined by Fick's second law. By replacing the exact series solution of Fick's second law (*2*, *3*) by a satisfactory empirical equation, Vermeulen (*11*) obtained the following breakthrough equation:

$$C/C_0 = (1 - \exp -[\theta - \Sigma + 0.614])^{\frac{1}{2}} \qquad (1)$$

Data conforming to this equation should produce a straight line when plotted as $\log [1 - (C/C_0)^2]$ vs. ΔY. The slope of the line is the internal mass transfer coefficient.

The internal mass transfer coefficient is defined as $k_p s = (4\pi^2 D_s)/(d_p^2)$. Generally it has been assumed that D_s which is the proportionality constant in Fick's second law is a function only of the cations being exchanged* and of temperature (*3*). Hence for a given isothermal ion exchange system $k_p s$ is a function only of resin particle size.

The formation of the constant-pattern exchange zone upon which Equation (1) is based requires a certain minimum bed length corresponding to $\Sigma = 4$. For beds shorter than this minimum required length the material-balance equation becomes more complicated and so therefore does the breakthrough equation. For this situation Vermeulen (*11*) has employed an empirical approximation to replace the exact solution to the differential equation formed from the material balance, equilibria, and rate relationships. The solution is presented as generalized breakthrough curves relating the effluent concentration to Σ and θ. These curves may be used for matching with experimental curves to determine whether the experimental data conform to the breakthrough equation. The internal diffusion transfer coefficient may then be evaluated from the curve parameters when correspondence is found.

EXPERIMENTAL PROCEDURE

Ferric perchlorate solutions prepared from a reagent-grade chemical were used as the exhausting solutions, since a previous study (Part I) had found that iron complexes were essentially completely absent in such solutions. Therefore exchange of only a single iron-containing ion, Fe^{+++}, occurs. Most regenerations were made with $2N$ hydrochloric acid. Dowex-50, $X - 8$ was employed. The resin was back washed to remove fines and was pretreated and tested for capacity and water content as described previously.

Experimental runs were made by passing solutions of known compositions into beds of ion exchange material at controlled flow rates. The beds were mounted in 1.13-mm. I.D. Pyrex glass tubes. The upper end of each tube was closed with a sintered-glass disk, and the lower end of the bed was

---

*More recent studies indicate that D_s should also be a function of resin composition (*6*,*7*), although no evidence of this was found in the present study.

Table 1. Calculated Values of K_ps

Run	C_0, meq./ml.	Flow rate, ml./(min.) (sq. cm.)	Bed depth, cm.	Σ found by curve matching	K_ps (1/hr.) calculated	Σ calculated for $K_ps = 33$
1–5	Preliminary runs					
6	1	5	25.5	—	26	4.06
7	1.0	14.8	25.5	1.5	36.6	1.35
8	1.0	26.5	25.5	0.85	36.4	0.77
9	1.0	45	25.5	0.6	46.0	0.45
10	1.25	15	25.5	1.0	30.5	1.08
11	2.0	15	25.5	0.71	34.6	0.628
12	2.0	14	45.5	0.8	20.0	1.33
13	1.15	15	45.5	2.0	28.2	2.33
14	0.51	14	25.5	3.0	35.0	2.83
15*	0.81	15	25.5	—	124	
16	0.51	15	45.5	—	33	4.90
17	0.51	24	61	—	33	4.2
18	0.4	15	61	—	33	7.7

*This run was made with 50- to 100-mesh–size resin particles.

supported by a glass-wool plug, which also served as a distributor. To minimize mixing within the solution after passage through the bed, the entire space between the glass-wool plug and sintered glass was filled with resin, and the effluent line above the bed was held to a minimum volume. To minimize mixing between the incoming solution and the water initially present in the bed from previous washings, all runs were made upflow, and the free volume between the individual feed lines and the bottom of the bed was held to a minimum. Because of the sintered-glass disk at the top of the bed, upflow runs could be made at high velocities without fluidizing the bed. In the preparation and use of the bed care was taken to ensure the absence of any entrapped air. Solutions were led to and from the bed through Tygon tubing and glass fittings, and the flow rate was controlled at the outlet. All effluent from the bed was collected in small samples, either manually or by use of a mechanically rotated collection table. The samples were subsequently analyzed for iron content colorimetrically, with potassium thiocyanate as the reagent.

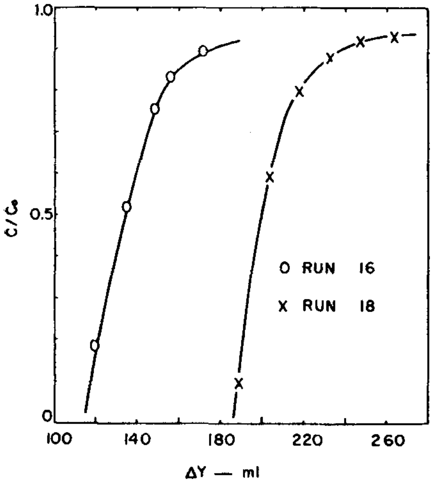

Fig. 1. Typical breakthrough curves for long beds; C/C_0, ratio of effluent to influent iron concentration, vs. ΔY, the effluent from bed (corrected for bed holdup).

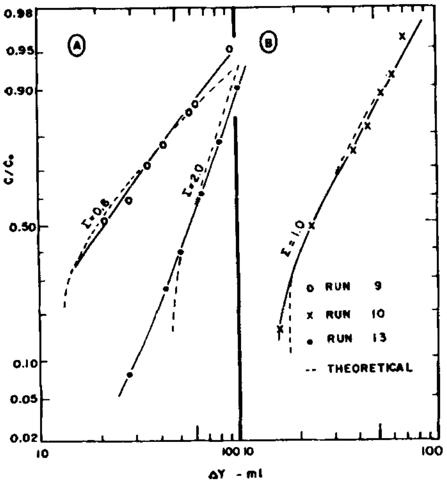

Fig. 2. Example of curve matching with generalized graphical solution of Vermeulen.

Following saturation of the bed with iron, the bed was washed, regenerated until the effluent gave no test for iron, and rewashed until the wash-water effluent was neutral to litmus paper. Washings and regenerations were also performed upflow.

Three different bed lengths, 25.5, 45.5, and 61 cm. were used. Flow rates ranged from 5 ml./min.-sq. cm. to 45 ml./min.-sq. cm. Influent exhaustion solutions were from 0.5 to 2.0 *N* in Fe^{+++}. Most runs were made with 20- to 50-mesh resin particles, but in one run 50- to 100-mesh particles were used. All runs were at approximately 24°C. A summary of the operating conditions in the various runs is included in Table 1.*

RESULTS

Typical breakthrough curves for the takeup of iron are shown in Figures 1 and 5. The trailing upper ends of the curves are characteristic of breakthrough curves when internal diffusion is the rate-controlling step. The lower ends of the curves should start almost vertically if rate-affecting factors other than internal diffusion were completely absent. The formation of constant pattern conditions may be noted by comparing the curves for runs 16 and 18, which differed only in bed lengths used.

For runs in which Σ was less than 4, the breakthrough curves were compared with curves on the generalized plot presented by Vermeulen (Figure 2). The plot is made on semilog probability paper. As shown in Figure 2, matching was usually obtained for C/C_0 values greater than approximately 0.2, so that the upper 80% of the curves matched. Values of k_ps were then determined from the values of Σ for the matching curves. These values are given in Table 1, and it may be noted that for the same particle size of resin the values of k_ps show only moderate variation in view of the curve-matching method employed.

The data from typical runs in which $\Sigma \geqq 4$ were plotted as log $[1 - (C/C_0)^2]$ vs. ΔY and as demanded by Equation (1) provided straight lines as shown in Figure 3. The values of k_ps given by the slopes of these lines are also listed in Table 1 and show very good agreement among themselves and with k_ps's computed by the curve-matching method.

DISCUSSION

In runs 6 through 9 the flow rate was varied, while other operating variables were held constant. In all but one of the subsequent runs (run 17) the flow rate was maintained constant, while either the entering solution was varied in iron content (0.5 *N* to 2.0 *N*) or the bed size was changed (25.5 to 61 cm.) Despite the ninefold velocity change and the above-listed changes in other variables, the experimental data for all but the very first portion of the breakthrough curves could be interpretated on the assumption that the only resistance to mass transfer is within the solid phase and that the equilibrium is essentially irreversible, as is indicated by the constancy of the k_ps values for the 20- to 50-mesh–size beds. To test further the conclusion that internal diffusion was the rate-controlling step, resin particles of 50- to 100-mesh size were used in run 15. For solid diffusion as the rate-controlling step k_ps should vary inversely as the square of the particle diameter (*3*). Average particle sizes for the 20- to 50-mesh- and the 50- to 100-mesh–size beds were found by particle-size measurements to be 0.56 and 0.28 mm. respectively. For these particle sizes and a k_ps of 33 for the 20- to 50-mesh–size particles, the predicted value of k_ps for the 50- to 100-mesh–size particles is 132. The experimentally determined value was 124, which is in very good agreement with the predicted value. An approximate value of D_s can be calculated from this equation for the average resin-particle diameter of 0.056 cm. and a k_ps of 33 1/hr. (9.16×10^{-3} 1/sec.). The calculated value of D_s is 7.6×10^{-7} sq. cm./sec. The self-diffusion coefficients

---

*A complete tabulation of original data and results is available in the Ph.D. thesis of R. C. Vasishth, University of Washington, Seattle, Washington, Seattle, (1958).

of some trivalent ions reported are Y^{+++} 9×10^{-9} sq cm./sec. (*10*) and Ce^{+++} 9.4×10^{-9} sq. cm./sec. (*4*). These are considerably smaller than the values calculated for the present studies. However Selke (*8*) has reported that for cations replacing H^+ the values of interdiffusion coefficients are considerably higher than the self diffusion coefficients, probably because of the very high diffusivity of the hydrogen ions.

The failure of the first portions of the experimental breakthrough curves to show the vertical rise at $C/C_0 = 0$, called for by theoretical considerations when internal diffusion is rate controlling, could be caused by either longitudinal mixing within the bed or by liquid-film resistance to mass transfer being important during the early part of the breakthrough. The latter might be anticipated because of the low concentration of iron in solution during this portion of the breakthrough (*3*, *5*). However attempts to correlate the data from the first parts of runs 6 through 9 on the basis of a liquid-film rate-controlling mechanism (*5*) were unsuccessful. To test the effects of longitudinal mixing within the bed, two runs were made in which a 1*N* iron solution was passed in the same manner as in ordinary exhaustion runs through a bed already saturated with iron. The results are shown in Figure 4. Although the width of the breakthrough curves for these two runs is narrow compared with ordinary exhaustion runs, the longitudinal mixing effects are sufficient to prevent formation of the vertical breakthrough curve which should be present for these runs with no longitudinal mixing in the bed.

The equations presented by Vermeulen are based on a completely irreversible equilibrium. The equilibrium data for $Fe^{+++} - H^+$ exchange at the concentrations used in the present study (see Part I) show that while the take-up of iron on the resin is highly favored, the equilibrium is not completely irreversible. However, when the equilibrium is as favorable as it is for iron take-up in the present system, for practical purposes the equilibrium may be treated as irreversible (*5*).

CONCLUSIONS

The match between the experimental breakthrough curves and theoretically predicted breakthrough curves and the consistency of the $k_p s$ values found for the experimental runs both support the conclusion that the ion exchange rate under the conditions of the present study is controlled by the diffusion rate within the pores of the resin particles. Although the flow rates used in the study ranged only from 1.23 to 11.1 g./(min.)(sq. ft.) of bed cross section, and the flow rates used industrially in ion exchange beds are often higher than these, higher flow rates should tend only to accentuate the rate-controlling importance of diffusion within the particles (*3*, *8*).

Back calculations also support the conclusion that the equations proposed by Vermeulen, equations based on internal diffusion being rate controlling and an irreversible equilibrium, represent well the major portion of the breakthrough curve for the system studied. Use of these equation with $k_p s = 33$ to back calculate some of the breakthrough curves from the present study is shown in Figure 5. Although the equations do not predict the first portion of the breakthrough curve because of longitudinal mixing effects within the bed, it was found that a reasonable approximation of this part of the curve could be obtained by the extrapolation of the breakthrough curve above C/C_0 of 0.2 on down to C/C_0 of 0. Accordingly it is felt that the equations can be used to predict breakthrough curves and to design commercial ion exchange units for the system studied or for similar systems for which the necessary basic data are available.

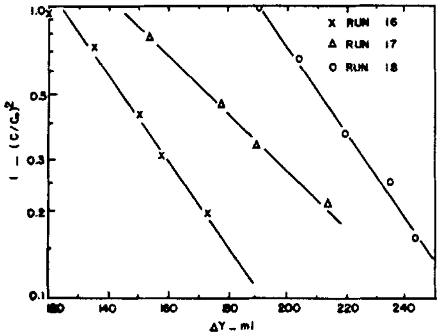

Fig. 3. Breakthrough data for long beds plotted according to Equation (1).

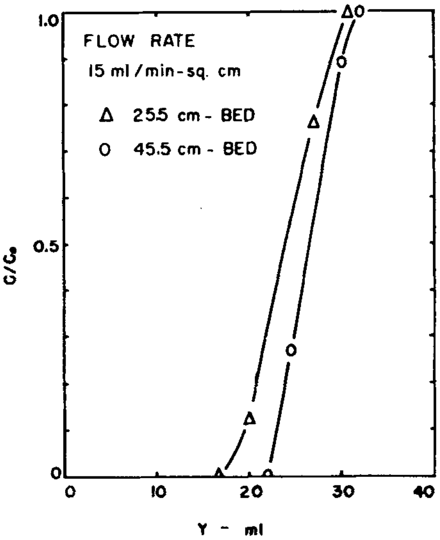

Fig. 4. Effects of longitudinal mixing on breakthrough curves.

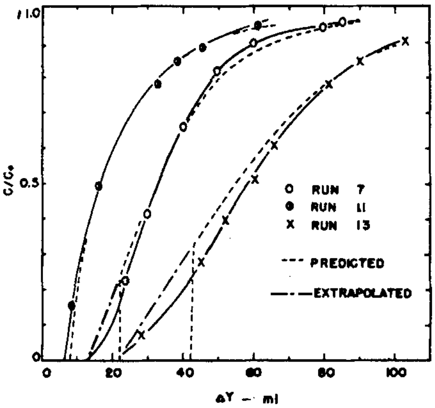

Fig. 5. Comparison of experimental and predicted breakthrough curves.

NOTATION

a = resin capacity, meq./g. dry hydrogen-form resin
C = concentration in effluent solution of the ion exchanging onto the resin, meq. iron/ml.
C_0 = concentration in entering solution of the ion exchanging onto the resin meq. iron/ml.
d_p = mean diameter of the resin particles, cm.
D_s = effective diffusivity of the exchanging ions in the resin phase, sq. cm./hr.
$k_p s$ = internal diffusion transfer coefficient = $(4\pi^2 D_s)/d_p^2$, 1/hr.
K = equilibrium constant
q = resin composition, meq. iron/g. dry hydrogen-form resin
R = flow rate through the bed, ml./hr.
v = volume of bed, ml.
ΔY = volume throughput corrected for the bed holdup, ml.
θ = $(k_p s \, \Delta Y)/R$, dimensionless
ρ = superficial resin density, g./ml.
Σ = $(k_p s a \rho v)/C_0 R$, dimensionless

LITERATURE CITED

1. Arehart, T. A., J. C. Bresee, C. W. Hancher, and S. H. Jury, *Chem. Eng. Progr.*, **52**, No. 9, 353 (1956).
2. Barrer, R. M., "Diffusion In and Through Solids," p. 29, University Press, Cambridge, England (1941).
3. Boyd, G. E., A. W. Adamson, and L. S. Myers, Jr., *J. Am. Chem. Soc.*, **69**, 2836 (1947).
4. *Ibid.*, **72**, 4807 (1950).
5. Hiester, N. K., S. B. Radding, R. L. Nelson, and Theodore Vermeulen, *A.I.Ch.E. Journal*, **2**, No. 3, 404 (1956).
6. Mar, W. A., and M. M. David, *ibid.*, p. 381 (1956).
7. Schlogl, R., and F. Helferich, *J. Chem. Phys.*, **26**, No. 1, 5 (1957).
8. Selke, W. A., Y. Bard, A. D. Pasternak, and S. K. Aditya, *A.I.Ch.E. Journal*, **2**, 468 (1956).
9. Selke, W. A., *Chem. Eng. Progr.*, **53**, No. 12, 601 (1957).
10. Soldano, B. A., *Ann. N. Y. Acad. Sci.*, **57**, 116 (1953).
11. Vermeulen, Theodore, *Ind. Eng. Chem.*, **45**, 1664 (1953).

Manuscript received June 30, 1958; revision received February 16, 1959; paper accepted March 23, 1959. Paper presented at A.I.Ch.E. Salt Lake City Meeting.